2018

Coherent terahertz Smith-Purcell radiation from Dirac semimetals grating with very deep and narrow slits

Tao Zhao
University of Electronic Science and Technology of China

Min Hu
University of Electronic Science and Technology of China

Zhen Lian
University of Electronic Science and Technology of China

Renbin Zhong
University of Electronic Science and Technology of China

Sen Gong
University of Electronic Science and Technology of China

See next page for additional authors

Coherent terahertz Smith-Purcell radiation from Dirac semimetals grating with very deep and narrow slits

Abstract

We demonstrate a physical mechanism of multicolor coherent terahertz (THz) Smith-Purcell radiation from surface plasmon polaritons (SPPs). In Dirac semimetals gratings with very deep and narrow slits, two types of SPP modes, the cavity and ordinary SPP modes, can be excited by fast electrons under different excitation conditions and then diffracted into radiation in specific directions. The radiation intensity is remarkably enhanced when SPPs are excited, and frequencies can be widely tuned by adjusting the parameters of grating and electrons. Our findings could provide a promising way for developing room temperature, coherent, tunable, directional, and intense THz radiation sources.

Disciplines

Engineering | Science and Technology Studies

Publication Details

Zhao, T., Hu, M., Lian, Z., Zhong, R., Gong, S., Zhang, C. & Liu, S. (2018). Coherent terahertz Smith-Purcell radiation from Dirac semimetals grating with very deep and narrow slits. Applied Physics Express, 11 (8), 082801-1-082801-4.

Authors

Tao Zhao, Min Hu, Zhen Lian, Renbin Zhong, Sen Gong, C Zhang, and Shenggang Liu

OPEN ACCESS

Applied Physics Express **11**, 082801 (2018)

https://doi.org/**10.7567/APEX.11.082801**

Coherent terahertz Smith–Purcell radiation from Dirac semimetals grating with very deep and narrow slits

Tao Zhao[1*], Min Hu[1], Zhen Lian[1], Renbin Zhong[1], Sen Gong[1], Chao Zhang[1,2], and Shenggang Liu[1]

[1]*Terahertz Research Center, School of Electronic Science and Engineering, University of Electronic Science and Technology of China, Chengdu, Sichuan 610054, China*

[2]*School of Physics and Institute for Superconducting and Electronic Materials, University of Wollongong, Wollongong, NSW 2522, Australia*

[*]E-mail: forzhaotao@uestc.edu.cn

Received April 28, 2018; accepted June 15, 2018; published online July 3, 2018

We demonstrate a physical mechanism of multicolor coherent terahertz (THz) Smith–Purcell radiation from surface plasmon polaritons (SPPs). In Dirac semimetals gratings with very deep and narrow slits, two types of SPP modes, the cavity and ordinary SPP modes, can be excited by fast electrons under different excitation conditions and then diffracted into radiation in specific directions. The radiation intensity is remarkably enhanced when SPPs are excited, and frequencies can be widely tuned by adjusting the parameters of grating and electrons. Our findings could provide a promising way for developing room temperature, coherent, tunable, directional, and intense THz radiation sources.

Since its first observation in 1953, by electrons passing over a periodic structure,[1)] Smith–Purcell radiation (SPR) has attracted tremendous interest for its possible applications in radiation generation, beam acceleration, and nondestructive diagnostics of electron beams.[2–5)] Its dispersion relation is as follows.

$$\lambda = -\frac{L}{n}\left(\frac{1}{\beta} - \cos\theta\right), \tag{1}$$

where λ is the wavelength of the radiation, n is the order of the radiation, L is the grating period, β is the ratio of the electron velocity to the speed of light, and θ is the observation angle [shown in Fig. 1(a)].

A diffraction model was applied to accurately explain the mechanism of SPR, as presented by van den Berg.[6–8)] The gratings were treated as perfectly conducting in many theoretical and experimental studies. However, finite conductivity should be considered in the optical region due to the possible excitation of the surface plasmon polaritons (SPPs) on the grating surface. The radiation can be significantly enhanced by 2 or 3 orders in particular angles when the phase-matching condition for the excitation of SPP mode is satisfied.[9,10)] In recent past, some studies demonstrated coherent THz SPR from SPPs on a graphene surface.[11–13)] This mechanism is expected to meet the urgent requirement of a room temperature, miniature, tunable, coherent, and high powered THz radiation source covering the whole THz regime. The desired THz radiation can be developed owing to the remarkable properties of graphene SPPs, such as extremely high confinement, low Ohmic loss, and more importantly, wide tunability in the THz to mid-infrared regimes by adjusting the gate voltage or chemical doping.[14–18)]

Recent experimental discovery of Cd_3As_2,[19–21)] Na_3Bi,[22)] and $ZrTe_5$[23)] demonstrated fermion quasiparticles with linear dispersion along all the three momentum directions. Thus, the three-dimensional (3D) Dirac semimetals, also called bulk Dirac semimetals (BDSs), can be viewed as the 3D counterparts of graphene. Similar to graphene, BDSs can also support SPPs in the THz to mid-infrared regimes. However, for the BDSs, the crystalline symmetry protection against gap formation results in much higher mobility.[24)] This may lead to lower intrinsic loss of SPPs in BDSs. An extra dimension facilitates the BDSs to form a 3D plasmonic grating, thus, supporting not only the ordinary SPP mode on the grating surface, but also the cavity SPP mode in the slits. Some studies on the plasmon mode in BDSs have also been performed earlier.[25–30)] Das Sarma et al. found that the plasmon frequency in a doped massless Dirac plasma was explicitly

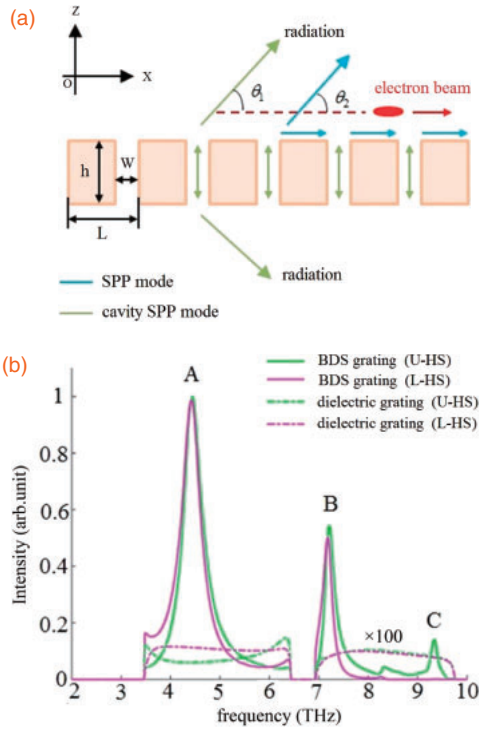

Fig. 1. (a) Schematic of the coherent SPR from BDS grating, θ indicates the radiation direction. (b) Fourier spectra of radiation intensity from BDS grating and dielectric grating (the geometric size is $L = 20\,\mu m$, $h = 15\,\mu m$, $w = 1\,\mu m$). The parameters of BDS: T is 300 K, τ is 1.2 ps, v_F is 9×10^5 m/s, g is 4, μ_c is 0.1 eV, and ε_∞ is 13. The beam velocity is $0.3c$. The permittivity of dielectric grating is 2.25. The radiation intensity of dielectric grating is scaled by 100 times. U-HS (L-HS) means the radiation towards to upper (lower) half-space.

nonclassical in all dimensions with the plasma frequency being proportional to $1/\sqrt{\hbar}$ in the long-wavelength range.[25] The universality of plasmon excitation with frequency in the THz range in the BDSs was discovered by Kharzeev et al.[26] The behavior of SPP and electromagnetic waves in BDS films with their Fermi level higher than the Dirac point and the role of the dielectric response in BDSs were studied earlier.[28]

In this letter, a physical mechanism explaining the multi-color coherent THz SPR from two types of SPP modes in a Dirac semimetals grating with very deep and narrow slits is presented. We show that the cavity and ordinary SPP modes have essential differences in the excitation conditions and radiation characteristics. Firstly, the excitation of cavity SPP mode must satisfy both the phase-matching and Fabry–Pérot (FP) resonance conditions, while, for the ordinary SPP mode, meeting the phase-matching condition is sufficient. Secondly, the radiation from cavity SPP mode occupies both the upper and lower half-spaces, while its counterpart occupies only the upper half-space. Finally, although the radiation intensities of the two kinds of SPP modes are significantly enhanced, the radiation power density of cavity SPP mode is much higher than that of the ordinary SPP mode. The underlying physics of these differences is uncovered.

The BDS grating has a period L, thickness h, and slit width w, as shown in Fig. 1(a). An electron beam moves parallel at a constant velocity v_0 in the x-direction above the grating surface at a distance z_0. The conductivity of BDSs derived by the Kubo formalism is given as[28]

$$\sigma(\omega) = \frac{ie^2}{\hbar}\frac{g}{6\pi^2 v_F \hbar^2}\frac{\mu_c^2 + (k_B T)^2/3}{\omega + i\tau^{-1}}, \tag{2}$$

where T, k_B, τ, v_F, g, and μ_c are the temperature, Boltzmann constant, relaxation time, fermion velocity, degeneracy factor and chemical potential, respectively. Here, only the intraband conductivity, which dominates the low frequency process of SPP, is included. The dielectric function of BDSs can be expressed through the dynamic conductivity: $\varepsilon_{BDS}(\omega) = \varepsilon_\infty + \sigma(\omega)/\omega\varepsilon_0$. ε_∞ is the dielectric constant at infinite frequency and ε_0 is the permittivity of vacuum.

The theoretical and numerical calculations are based on the rigorous coupled-wave analysis (RCWA) method, which is commonly used to analyze the diffraction problem of grating with or without SPPs.[13,31,32] Figure 1(b) shows the radiation spectra in the THz frequency regime. There are three obvious radiation peaks, marked by the frequency points A, B, and C, in the radiation regime of the first and second negative space harmonics ($n = -1$ and -2), the frequencies are 4.42 THz, 7.22 THz, and 9.34 THz, respectively. The radiations at frequency points A and B emit into both the upper and lower half-spaces, while the radiation at frequency point C emits only into the upper half-space. In addition, the radiation intensity at frequency points A and B is much higher than that at frequency point C. To uncover the mechanisms of THz generation and related physical phenomena, we calculate the distribution of magnetic field intensity of radiation at frequency points A, B, and C, as shown in Fig. 2. The radiation angles satisfying the dispersion Eq. (1) are 93°, 145°, and 83°, for A, B, and C, respectively. Strong resonances are observed in the slits for frequency points A and B, while for the frequency point C, the SPPs exist on the upper surface of the grating. Thus, from the first glimpse, we may conclude that the coherent SPR is generated from the cavity mode in the slits and the ordinary SPP mode based on the SP effect.

To give a further insight into the physics of SPR and the formation of the cavity mode, we calculate the eigen modes of the grating region at the resonant frequencies. For the RCWA method, the fields in the grating region are expanded into infinite terms of eigen modes $e^{(\pm q_p z)}$, q_p is the p-th eigen mode.[31,32] The results indicate that there exists an SPP eigen mode, which dominates the fields in the grating region. The SPPs are indeed formed by strong coupling of surface charges on the two opposite sides of a grating slit. This is confirmed by the SPP dispersion of single slit with infinite thickness, as given in Eq. (3).[33,34] Although a finite thickness of grating slits is considered, the SPP eigen mode is closely fitted to the dispersion relation given below.

$$\tanh\left(\frac{w}{2}\sqrt{k_{SPP}^2 - k_0^2}\right) = -\frac{1}{\varepsilon_{BDS}}\sqrt{\frac{k_{SPP}^2 - \varepsilon_{BDS}k_0^2}{k_{SPP}^2 - k_0^2}}, \tag{3}$$

where k_{SPP} is the wavevector of the cavity SPP mode along the slits (z-direction), $k_0 = \omega/c$, c is the velocity of light in vacuum.

The cavity resonance of SPPs in the slits can occur only when both the FP and phase-matching conditions, given in Eqs. (4)[33,34] and (5)[9,10] are satisfied, which is essentially different from that of the ordinary SPP mode.

$$q_{SPP}h + \phi_R = m\pi, \tag{4}$$

where q_{SPP} is the eigen value of SPPs in the grating region and ϕ_R is the phase shift associated with reflection of cavity SPP mode at the slits end facet. m is an integer indicating the order of FP resonance. The cavity SPP modes at frequency points A and B are corresponding to the first and second orders ($m = 1$ and 2) of FP resonant modes, the numerical fitted ϕ_R are $0.1 \times 1\pi$ and $0.1 \times 2\pi$, respectively.

$$\omega/v = k_{SPP}^x, \tag{5}$$

where v is the velocity of the electron beam, k_{SPP}^x is the wavevector of SPPs along the direction of moving electrons (x-direction).

The SPPs are propagating up and down along the side walls and reflecting at the slits end facets back to the resonance cavity. The cavity retains most of the energy of SPPs and leaks the remainder part to the diffraction fields by the SP effect at the openings of the slits. The propagating feature of SPPs in the slits guarantees the radiation to occur both in the upper and lower half-spaces. In contrast, the ordinary SPP mode located on the grating surface can only be radiated into upper half-space because the SPPs cannot penetrate the thick enough grating to reach the lower grating surface.[33,34]

After having understood the physical mechanism of coherent THz SPR from a BDS grating, we now deal with the enhancement of the radiation power density by SPPs. According to the diffraction model, the evanescent wave generated by the electron beam can be diffracted into an incoherent radiation. This conventional SPR is chosen as the control group, and a dielectric grating that cannot support SPPs, is preferred owing to its numerical compatibility with the plasmonic grating. Figure 1(b) shows the radiation spectra with and without excitation of SPPs. The radiation power density is enhanced by 1347, 986, and 224 times at the

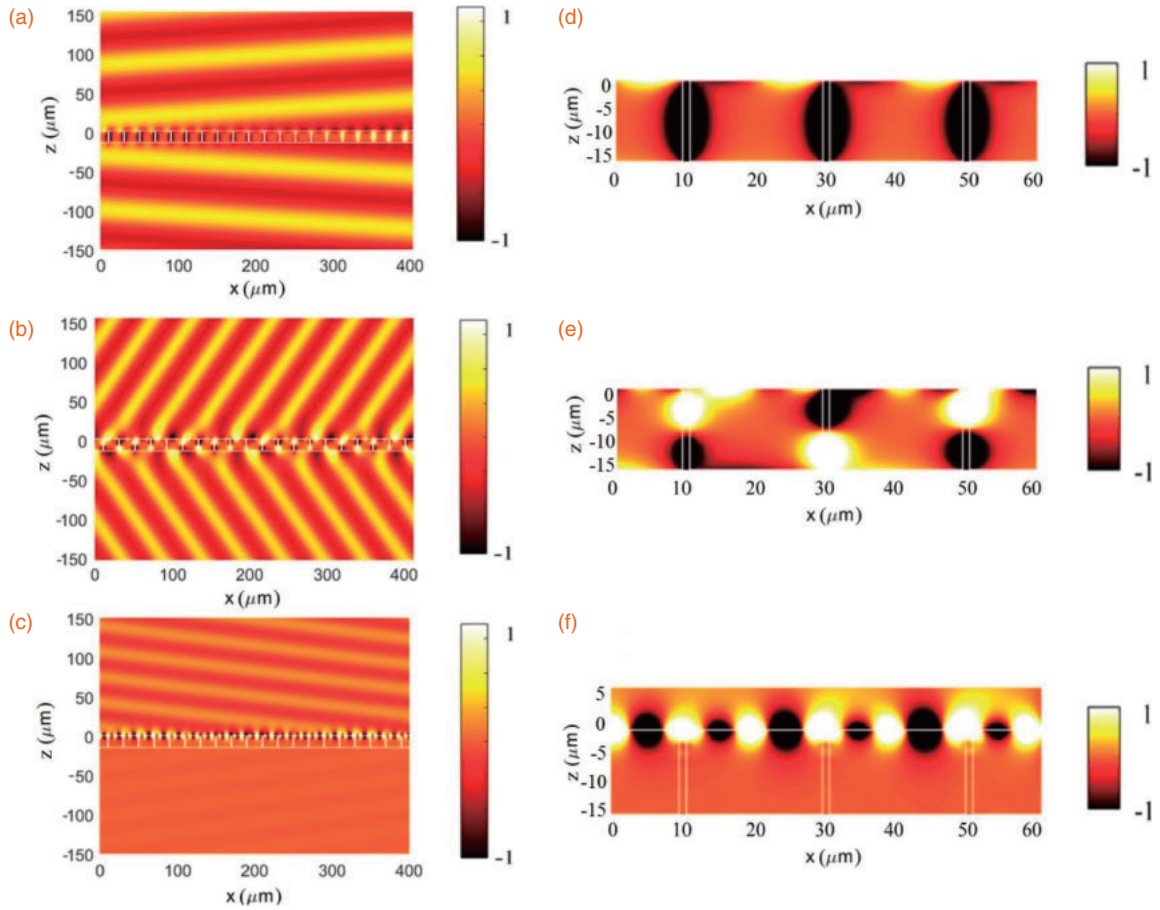

Fig. 2. The contour maps of magnetic field intensity H_y in the X–Z plane of the structure for frequency points A, B, and C, respectively. (d)–(f) indicate the fields in the grating region.

SPP resonance frequency points A, B, and C, respectively, due to the strong local fields. The intensity of SPPs field excited by the electron beam is two or three orders of magnitude higher than that of the evanescent wave and this is the physical origin of the large enhancement. This leads to much stronger diffraction fields. For an electron beam with a charge density 100 pC/cm, the peak radiation power density can reach 1.26×10^4, 1.69×10^3, and 0.73×10^3 W/cm^2. The highest radiation density in this case is one order higher than that from graphene SPPs in a grating structure.

The radiation from cavity SPP mode is more intense than that from the ordinary SPP mode, the ratios of radiation power density between frequency points A or B and C reach 17 and 2.3, respectively. The fields distribution in the grating region shown in Figs. 2(d)–2(f) indicate the comparable intensity of cavity and ordinary SPP modes. Thus, the powered radiation at frequency point A may explain the fact that the radiation is diffracted from the first negative space harmonic of SPPs with more energy than the second negative space harmonic. Although the radiations at frequency points B and C are both transformed from the second negative space harmonic of SPPs, more intense radiation of cavity SPP mode manifests that energy of cavity mode is diffracted more.

The grating slits play a key role in the cavity SPP resonance. We now analyze the influence of the grating slits on the radiation frequency of cavity SPP mode. Figure 3 shows the dependence of radiation frequencies of the first and second cavity modes on the thickness and width of the grating slits. When these two parameters are varied, the beam energy is adjusted to meet the excitation conditions. As the thickness increases, the radiation frequencies of both first and second cavity SPP modes decrease, obeying the FP relation, as shown

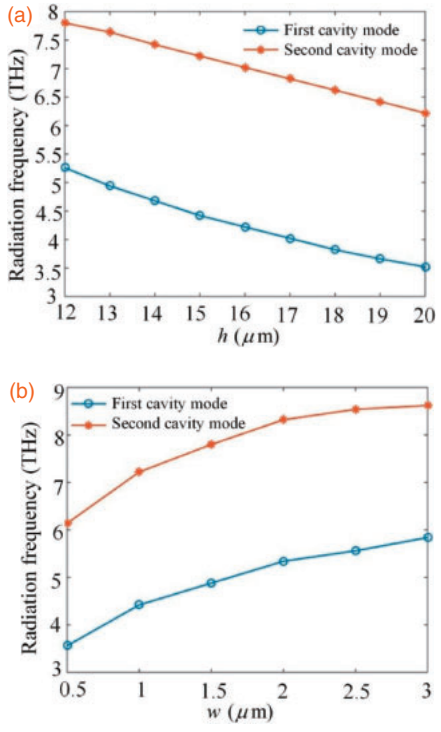

Fig. 3. The radiation frequencies of first and second cavity modes vs the grating height (a) and slit width (b).

in Fig. 3(a). Figure 3(b) reveals that as the width of the grating slits increases, the radiation frequencies of both the first and second orders cavity SPP modes increase. This can be explained by the dispersion equation [Eq. (3)]. The SPP energy will increase with decreasing slit width leading to higher radiation frequency.

In summary, we revealed physical mechanisms of multi-color coherent THz SPR from the cavity and ordinary SPP modes in a BDS grating with very deep and narrow slits. The essential differences of excitation conditions and radiation characteristics from these two SPP modes were analyzed. It was deduced that the excitation of cavity SPP mode needs an additional condition of FP resonance other than the phase-matching condition. The radiation from cavity SPP mode emits into both the upper and lower half-spaces, while the ordinary SPP mode emits only into the upper half-space. The radiation power density of cavity SPP mode could be significantly enhanced over three orders, up to $1.26 \times 10^4\,\mathrm{W/cm^2}$, which is one order higher than that of ordinary SPP mode. The radiation frequency of cavity SPP mode can be widely tuned by adjusting the grating parameters and beam energy. Therefore, based on this mechanism, room temperature, miniature, coherent, tunable, directional, and intense THz radiation sources covering the whole THz frequency band can be developed.

Acknowledgments This work was supported by the National Key Research and Development Program of China (2017YFA0701000); the Program 973 (2014CB339801); Fundamental Research Funds for the Central Universities (FRFCU) (ZYGX2016KYQD113); Natural Science Foundation of China (NSFC) (61231005, 11305030, 612111076, 61701084).

1) S. J. Smith and E. M. Purcell, Phys. Rev. **92**, 1069 (1953).
2) M. J. Moran, Phys. Rev. Lett. **69**, 2523 (1992).
3) M. Castellano, V. A. Verzilov, L. Catani, A. Cianchi, G. Orlandi, and M. Geitz, Phys. Rev. E **63**, 056501 (2001).
4) A. S. Kesar, Phys. Rev. Accel. Beams **13**, 022804 (2010).
5) P. A. Molenaar, P. van der Straten, H. G. M. Heideman, and H. Metcalf, Phys. Rev. A **55**, 605 (1997).
6) P. M. van den Berg, J. Opt. Soc. Am. **63**, 689 (1973).
7) P. M. van den Berg, J. Opt. Soc. Am. **63**, 1588 (1973).
8) P. M. van den Berg, J. Opt. Soc. Am. **64**, 325 (1974).
9) S. L. Chuang and J. A. Kong, J. Opt. Soc. Am. A **1**, 672 (1984).
10) N. E. Glass, Phys. Rev. A **36**, 5235 (1987).
11) S. G. Liu, C. Zhang, M. Hu, X. X. Chen, P. Zhang, S. Gong, T. Zhao, and R. B. Zhong, Appl. Phys. Lett. **104**, 201104 (2014).
12) T. Zhan, D. Han, X. Hu, X. Liu, S. Chui, and J. Zi, Phys. Rev. B **89**, 245434 (2014).
13) T. Zhao, R. B. Zhong, M. Hu, X. X. Chen, P. Zhang, S. Gong, and S. G. Liu, Chin. Phys. B **24**, 094102 (2015).
14) E. Hwang and S. Sarma, Phys. Rev. B **75**, 205418 (2007).
15) L. Ju, B. Geng, J. Horng, C. Girit, M. Martin, Z. Hao, H. Bechtel, X. Liang, A. Zettl, Y. Shen, and F. Wang, Nat. Nanotechnol. **6**, 630 (2011).
16) A. Vakil and N. Engheta, Science **332**, 1291 (2011).
17) M. Jablan, H. Buljan, and M. Soljačić, Phys. Rev. B **80**, 245435 (2009).
18) A. Grigorenko, M. Polini, and K. S. Novoselov, Nat. Photonics **6**, 749 (2012).
19) S. Borisenko, Q. Gibson, D. Evtushinsky, V. Zabolotnyy, B. Büchner, and R. J. Cava, Phys. Rev. Lett. **113**, 027603 (2014).
20) M. Neupane, S. Y. Xu, R. Sankar, N. Alidoust, G. Bian, C. Liu, I. Belopolski, T. R. Chang, H. T. Jeng, H. Lin, A. Bansil, F. Chou, and M. Z. Hasan, Nat. Commun. **5**, 3786 (2014).
21) Z. K. Liu, J. Jiang, B. Zhou, Z. J. Wang, Y. Zhang, H. M. Weng, D. Prabhakaran, S.-K. Mo, H. Peng, P. Dudin, T. Kim, M. Hoesch, Z. Fang, X. Dai, Z. X. Shen, D. L. Feng, Z. Hussain, and Y. L. Chen, Nat. Mater. **13**, 677 (2014).
22) Z. K. Liu, B. Zhou, Y. Zhang, Z. J. Wang, H. M. Weng, D. Prabhakaran, S.-K. Mo, Z. X. Shen, Z. Fang, X. Dai, Z. Hussain, and Y. L. Chen, Science **343**, 864 (2014).
23) Q. Li, D. E. Kharzeev, C. Zhang, Y. Huang, I. Pletikosic, A. V. Fedorov, R. D. Zhong, J. A. Schneeloch, G. D. Gu, and T. Valla, Nat. Phys. **12**, 550 (2016).
24) T. Liang, Q. Gibson, M. N. Ali, M. Liu, R. J. Cava, and N. P. Ong, Nat. Mater. **14**, 280 (2015).
25) S. Das Sarma and E. H. Hwang, Phys. Rev. Lett. **102**, 206412 (2009).
26) D. E. Kharzeev, R. D. Pisarski, and H.-U. Yee, Phys. Rev. Lett. **115**, 236402 (2015).
27) J. Hofmann and S. Das Sarma, Phys. Rev. B **91**, 241108(R) (2015).
28) O. V. Kotov and Yu. E. Lozovik, Phys. Rev. B **93**, 235417 (2016).
29) A. Thakur, R. Sachdeva, and A. Agarwal, J. Phys.: Condens. Matter **29**, 105701 (2017).
30) Ž. B. Lošić, J. Phys.: Condens. Matter **30**, 045002 (2018).
31) M. G. Moharam and T. K. Gaylord, J. Opt. Soc. Am. **71**, 811 (1981).
32) M. G. Moharam and T. K. Gaylord, J. Opt. Soc. Am. **72**, 1385 (1982).
33) J. Fiala and I. Richter, Plasmonics **13**, 835 (2018).
34) Y. Ding, J. Yoon, M. H. Javed, S. H. Song, and R. Magnusson, IEEE Photonics J. **3**, 365 (2011).